MDPI

Article

Magnetic Properties of Quasi-One-Dimensional Crystals Formed by Graphene Nanoclusters and Embedded Atoms of the Transition Metals

**Vladislav O. Cheranovskii [1],[*] , Viktor V. Slavin [2], Elena V. Ezerskaya [1],
Andrei L. Tchougréeff [3],[4],[5] and Richard Dronskowski [3],[6]**

[1] V.N. Karazin Kharkiv National University, Svoboda Sq.4, 61022 Kharkiv, Ukraine; cheranovskii@i.ua
[2] B.Verkin Institute for Low Temperature Physics and Engineering of the National Academy of Sciences of
Ukraine, 61103 Kharkiv, Ukraine; slavin@ilt.kharkov.ua
[3] Chair of Solid State and Quantum Chemistry, RWTH Aachen University, 52056 Aachen, Germany;
tch@elch.chem.msu.ru
[4] A.N. Frumkin Institute of Physical Chemistry and Electrochemistry of RAS, 199071 Moscow, Russia
[5] Independent University of Moscow, 119002 Moscow, Russia
[6] Jülich–Aachen Research Alliance, JARA-HPC, RWTH Aachen University, 52056 Aachen, Germany;
drons@HAL9000.ac.rwth-aachen.de
[*] Correspondence: cheranovskii@i.ua

check for
updates

Abstract: Using the density-matrix renormalization group method and quantum Monte Carlo simulation, we studied numerically the energy spectrum and thermodynamics of the quantum Heisenberg spin model for narrow graphene nanoribbons and their derivatives with periodically embedded heteroatoms. For several nanoribbon structures we found macroscopic ground state spin, gapless lowest excitation spectra and intermediate magnetization plateaus at low temperatures. We also studied the lowest energy states of frustrated systems formed by triangular graphitic clusters connected by bridged ions of transition metals. On the base of many-body perturbation theory and the exact diagonalization method, we showed the possibility of spin switching for this model due to the change the corresponding coupling parameters.

Keywords: graphene clusters; intermediate magnetization plateau; spin switching

1. Introduction

Finite strips of graphene, usually referred to as graphene nanoribbons, are very interesting subjects in the context of future spintronic applications of carbon-based materials [1,2] They are also the components of the numerous carbon allotropes as described in a comprehensive survey [3] and are shown recently to be an element of a tentative lowest energy carbon allotrope [4]. Although magnetic properties of carbon allotropes are not covered in the most comprehensive Samara Carbon Allotrope Database (SACADA) [5], the magnetically-ordered states in carbon-based materials were considered in the literature [6–8] before the experimental discovery of graphene and its related structures.

One of the most fundamental predictions for graphene nanoribbons is the possibility of spontaneous edge-state magnetism in the case of the ribbons with zigzag edges. This prediction is based on different mean field approximations like the unrestricted Hartree–Fock method [9–11] and density functional theory (DFT) [12]. It is known that these methods overestimate the spin polarization effects. On the other hand, more correct many-electron treatment of graphene nanoribbons within the Hubbard model, according to Lieb's theorem [13], gives singlet ground state and zero spin densities on the nanoribbon sites. This means that the electron correlation effects are crucial for correct description

of the magnetic properties of graphene nanoribbons [14]. Unfortunately, many electron studies of the magnetic structure of pristine graphene nanoribbons require large computational efforts and there are very few papers devoted to this problem [14–17].

Since the pristine nanoribbons have singlet ground state, the magnetic derivatives of this material have importance for the practical realization of spin-polarized electronic transport. It is found both theoretically and experimentally that atoms of transition metals (ATM) may fill carbon vacancies in graphene clusters to form stable ATM-embedded structures [18,19]. According to Lieb's theorem, structures with periodically embedded ATM may have macroscopic values of total spin in ground state with "ferrimagnetic" spin ordering. Another interesting hypothetic magnetic structure on the base of zigzag nanoribbons is so-called "carbon chain bridged graphene ribbons" considered in [20]. There is also theoretical proposal to create nanomagnets on the base of triangular-shaped finite graphene fragments (graphene nanoflakes) [21,22].

In contrast to pristine graphene nanoribbons, the theoretical description of the magnetic structure of these materials is based on different variants of DFT only. Therefore, many-electron consideration of the magnetic properties of above composite nanostructures on the base of graphene fragments is of interest. In our study for this purpose we used the Heisenberg spin Hamiltonian method [23–26]. This method permits us to treat not only pure π-electron systems like pristine graphene nanoribbons, but also to take into account interactions with other possible magnetic components e.g., transition metal ions of arbitrary spin. It also allows one to profit from available exact results concerning the energy spectrum and the ground state spin structure of bipartite spin systems. We use these results for the preliminary choice of the model spin structures on the base of graphitic clusters like nanoribbons and nanoflakes.

Note also, besides the numerous successful applications in solid-state physics, Heisenberg spin Hamiltonian is also treated as the spin formalism of known valence bond methods of quantum chemistry [27–29]. Unfortunately, this approach is not programmed in the existing solid-state quantum chemistry packages. We used idealized geometry for graphene clusters as the finite fragments of hexagonal lattice, because the main idea of our study is to give common many-electron descriptions of the low-temperature magnetic properties of the graphene-based nanostructures and compare these with known theoretical and experimental results.

Due to the exponential growth of the numerical difficulties, the exact diagonalization study of the Heisenberg spin model on the fragments of hexagonal lattice can be done only for relatively small lattice clusters. Therefore, for the detailed study of the proposed spin models we use combination of an approximate analytical approach: linear spin wave approximation (LSWA) and (exact) numerical methods: infinite and finite scheme of density matrix renormalization group (DMRG) [30] and the quantum Monte Carlo method (QMC) based on stochastic series expansion approach [31].

The paper is organized as follows: In the second Section, we give short description of spin lattice models for graphene nanoribbons with embedded ATM and consider general properties of the energy spectra and magnetic properties of these nanoribbons on the base of the known exact theorems for the bipartite Heisenberg spin systems. In the third Section, we present the results of our numerical and analytical studies of the lowest energy spectra and the field dependencies of magnetization at low temperatures for the spin lattice structures mentioned above. One of the most interesting results here is the unusual low-temperature effect: the intermediate plateau in field dependence of magnetization of narrow pristine zigzag nanoribbons and additional magnetization plateau for similar doped nanoribbons. We also analyze the possibility of spin switching for frustrated systems formed by triangular graphene clusters connected by bridged ions of transition metals with the help of many-body perturbation theory (PT). The details of the analytical spin wave study of the low-energy excitations of zigzag nanoribbons are given in the Appendix A.

2. Materials and Methods

All the spin lattice structures are described by the Heisenberg spin Hamiltonian

$$\mathbf{H} = \sum_{<i,j>} J_{ij} S_i S_j,$$

where J_{ij} is a coupling constant describing the interaction between spins located on the *i*-th and *j*-th lattice sites; S_i is an operator of *i*-th site spin.

In the present paper we are going to apply the above Heisenberg spin model for description of the tentative components of quasi-one-dimensional crystalline materials. One of the simplest tentative components are narrow graphene nanoribbons like polyacene (simplest zigzag-edged nanoribbon) and polyphenylene (armchair nanoribbon) macromolecules. According to Lieb theorem [32] these macromolecules have singlet ground state in the framework of Heisenberg. Their possible derivatives obtainable by a regular embedding of heteroatoms are presented in Figure 1a,b, respectively. Similar structures with embedded heteroatoms can be easily generated for nanoribbons of arbitrary width. For example, in the case of so called 3-zigzag graphenic nanoribbon [12] we have the derivative shown on Figure 1c.
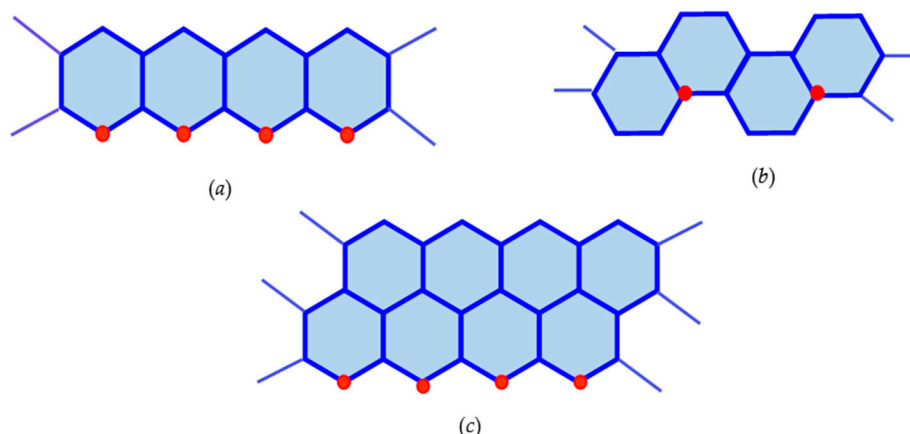

Figure 1. Fragments of the simplest magnetic nanoribbons with embedded heteroatoms (red balls). (**a**) Zigzag polyacene derivative; (**b**) armchair polyphenylene derivative; (**c**) 3-zigzag graphenic nanoribbon derivative.

The nanoribbons addressed in the present study (see Figure 1) are, so called, alternant or bipartite lattices. This means that the lattice sites can be divided into two subsets so A and B that sites of one subset have nearest neighbors only from another one (the corresponding coupling constants J_{ij} are nonvanishing). The ground state spin S_0 of alternant spin lattices satisfies the extended Lieb theorem [33], according to which $S_0 = |S_A - S_B|$, where S_A and S_B are the maximal values of total spin of sublattices A and B, respectively. It can be shown, that all our nanoribbon fragments formed by N unit cells have the ground state spin $S_0 = |s' - 1/2|N$ with no further degeneracy. Here s' is the spin of the embedded heteroatoms (red balls in Figure 1). Obviously, for nanoribbons of infinite length, S_0 takes macroscopic value if $s' \neq 1/2$. Moreover, according to the extended Lieb–Shultz–Mattis (LSM) theorem [34–37], the 1D alternant periodic spin systems with a macroscopic ground state spin which are similar to the above nanoribbon derivatives have no gap in the exact energy spectra at $s' \neq 1/2$.

In particular, the polyacene derivative (Figure 1a) with $s' = 0$ is equivalent to the so-called polyallyl spin chain [38], having macroscopic value of the ground state spin, gapless energy spectrum and intermediate plateau in the field dependence of magnetization at low temperature. We may expect similar properties for other narrow nanoribbons with embedded heteroatoms, but additional investigation is necessary.

Interesting possibilities for the design of magnetic materials on the base of nanoribbon fragments were proposed in [20]. Application of this idea to the nanoribbons decorated by magnetic heteroatoms leads to the following sandwich structures as shown in Figure 2.
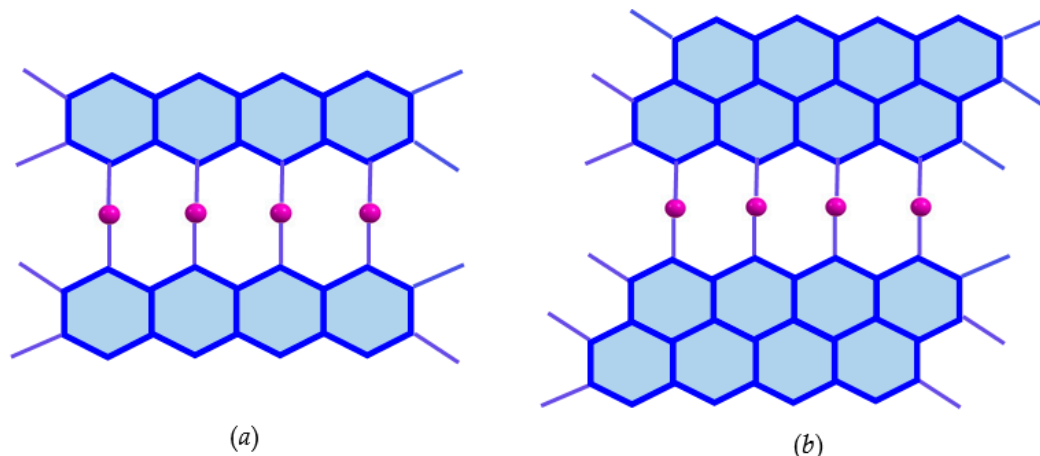

Figure 2. Composite structures on the base of two zigzag graphitic nanoribbons. The cases (**a,b**) correspond to the polyacene and 3-zigzag graphenic nanoribbon, respectively.

It can be easily shown that these structures have similar general characteristics of their exact energy spectra and the ground state spin structure as the zigzag nanoribbons with the embedded heteroatoms.

There is also a big family of magnetic structures on the base of small graphenic clusters (nanoflakes) connected by bridge magnetic atoms. Probably, one of the simplest representations of this type of structure is the high spin hydrocarbon *m*-polydiphenilcarbene [39] (see Figure 3 where the red balls represent carbon atoms in carbenic state, featuring $s' = 1$).
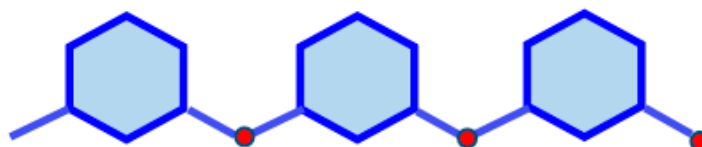

Figure 3. *m*-polydiphenilcarbene magnetic sublattice.

According to the extended Lieb theorem, substitution of the bridge carbon atoms by transition metal atoms with nonzero spins $s' \neq 0$ yields a bipartite spin chain system with macroscopic ground state spin.

There is an interesting possibility for the design of new magnetic materials on the base of triangular graphene clusters [21,22,24]. To combine this idea with the structural motif of polyphenilencarbene (Figure 3) we propose the frustrated spin chain system shown in Figure 4.
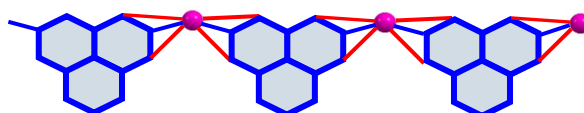

Figure 4. Model frustrated chain on the base of triangular graphitic clusters formed by 13 carbon atoms.

Additional nearest neighbor interactions should be taken into account in such a system since they can be relatively large due to multiple exchange paths [40] involving transition metals ions. On the other hand, the bridge between neighboring triangular clusters may have a more complicated structure (some additional ancillary ligands may be present at metal atoms, forming coordination compounds with nonzero spin).

3. Results

In order to predict magnetic properties of the tentative quasi-one-dimensional materials featuring the graphene-like components which may have different ground state spin depending on the spin of the embedded atoms (see previous section), we studied the spectra of their lowest energy excitations by linear spin wave (LSW) approximation for different values of s' (see Appendix A for technical details).

For big finite fragments of the zigzag nanoribbons formed by N unit cells (Figure 1a,c) with periodic boundaries and $s' \neq 1/2$ LSW gives the estimations for the lowest excitation energies $\varepsilon \sim N^{-2}$ (the details of the analytical calculations are given in Appendix A). This means, in the limit $N \to \infty$ these nanoribbons have a gapless excitation energy spectrum that is in agreement with the extended LSM theorem. For $s' = 1/2$ the LSW approximation yields the estimation $\varepsilon \sim N^{-1}$ (gapless energy spectrum for infinite nanoribbons). However, the case $s' = 1/2$ (including the ribbon of pristine polyacene itself) corresponds to zero value of ground state total spin of isolated unit cell. Therefore, it does not satisfy the conditions of the extended LSM theorem and additional studies are necessary.

In order to perform this, we used finite and infinite numerical schemes of the DMRG. Both demonstrate small finite energy gap ΔE in the lowest energy excitation spectrum (triplet excitations). This means that the LSW approach does not work properly for pristine polyacene. For $s' = 1$ the DMRG calculations gives gapless low-energy branches of the excitations that are in agreement with the LSM theorem and the LSW analytical estimation. To estimate ΔE more precisely we used a finite DMRG scheme and performed linear extrapolation of the energy gap value using the scaling law: $\Delta E_N = \Delta E + a/N$, where N is the number of optimized states (Figure 5a). We also used the QMC method to determine ΔE (Figure 5b). Within this approach, the gap is derived by numerically estimating the width of zero magnetization plateau then extrapolated to zero external magnetic field. The field dependencies of the magnetization at zero and low temperatures were very informative of characteristics of energy spectra structure [41]. This is why we paid special attention to studying these dependencies of the nanoribbons.
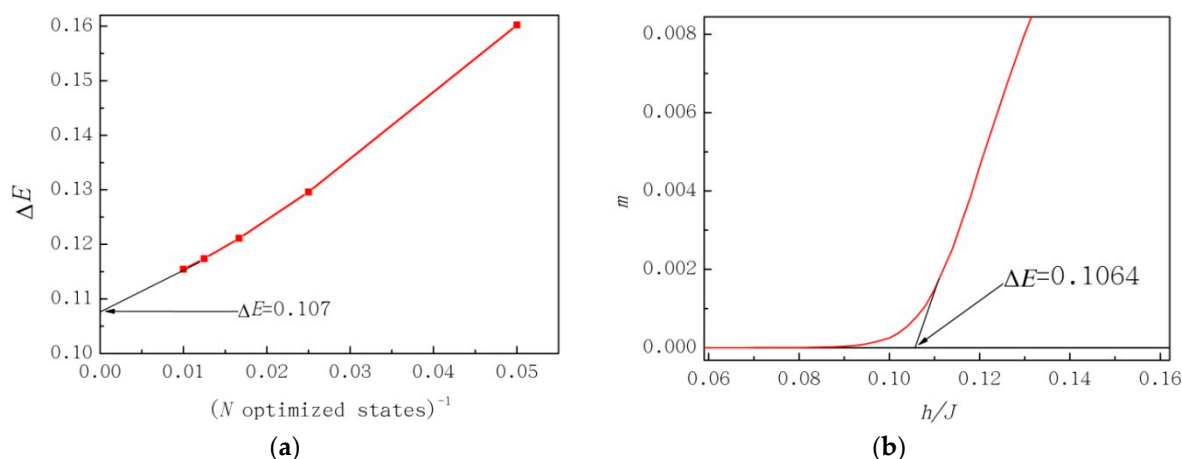

Figure 5. The estimations for the energy gap ΔE for pristine polyacene. Finite size DMRG method was used for the cluster of 400 spins (**a**) and QMC at temperature $T = 0.005$ J-for a cluster of 320 spins (**b**) were used.

In all our numerical calculations we put equal exchange constant between carbon spins $J_{ij} = J = 1$. The other quantities, such as J' (exchange constant between carbon spin and embedded spin s'), temperature T and external magnetic field h are measured in units of J.

For polyacene derivative with $s' = 1$ our DMRG calculations showed intermediate plateau of magnetization at $m = 0.125$ which agrees with the existence of gapped excitations of the total spin $S \geq S_0$ similar to the case of embedded spins with $s' = 0$ considered above. The presence of an additional intermediate plateau at $m = 0.25$ is even more intriguing. According to our DMRG and

QMC calculations for a cluster of 320 spins, the second plateau is also present in the pristine polyacene (Figure 6).
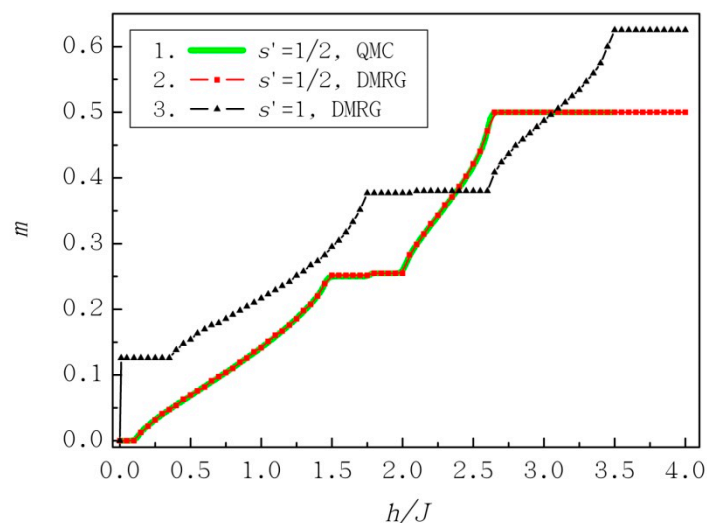

Figure 6. Intermediate plateau in the field dependence of the magnetization per spin *m* for the system Figure 1a for $s' = 1/2$ and $s' = 1$. The QMC simulation was carried out at the temperature $T = 0.01\,J$, the DMRG one was carried out the number of optimized states $N = 50$.

According to our DMRG calculations this plateau is present because of the energy gap between the states with $S < S_{max}/2$ and the states with $S = S_{max}/2$.

It is of interest, that for the simplest pristine armchair nanoribbon (Figure 1b) we did not find the intermediate magnetization plateau (Figure 7).
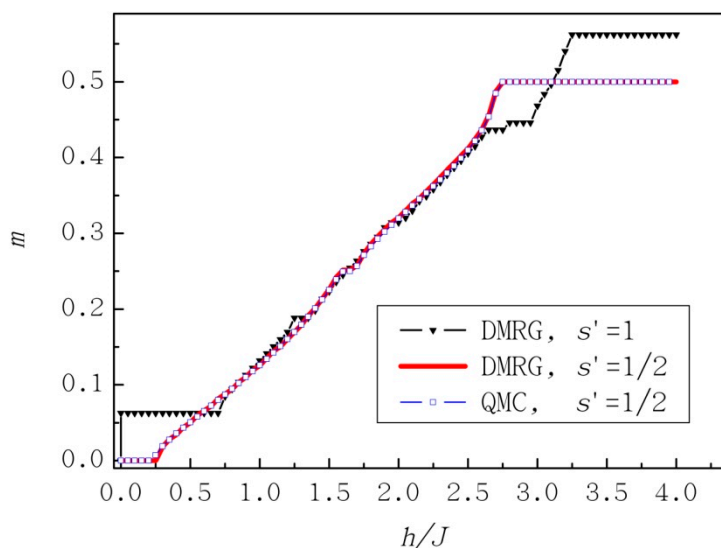

Figure 7. Field dependence of magnetization *m* for the cluster of 320 spins of the system shown on the Figure 1b, for $s' = 1/2$ and $s' = 1$. QMC: $T = 0.01\,J$, DMRG: $N = 50$.

We also studied numerically the field dependence of magnetization for a more complicated system: pristine 3-zigzag nanoribbon and the corresponding derivatives with embedded nonmagnetic heteroatoms shown in Figure 1c by the QMC method (the cluster of 648 spins; one spin per site).

According to these calculations (Figure 8) we have intermediate magnetization plateau only for the magnetic derivative similar to the case of polyphenylene (Figure 7). For the pristine 3-zigzag nanoribbon our QMC calculations demonstrated the absence of the plateau with zero magnetization in

contrast to the case of pristine polyacene and polyphenilene. Probably, the pristine 3-zigzag nanoribbon has very small gap in the energy spectrum and the accuracy of our numerical study is not enough to determine this.
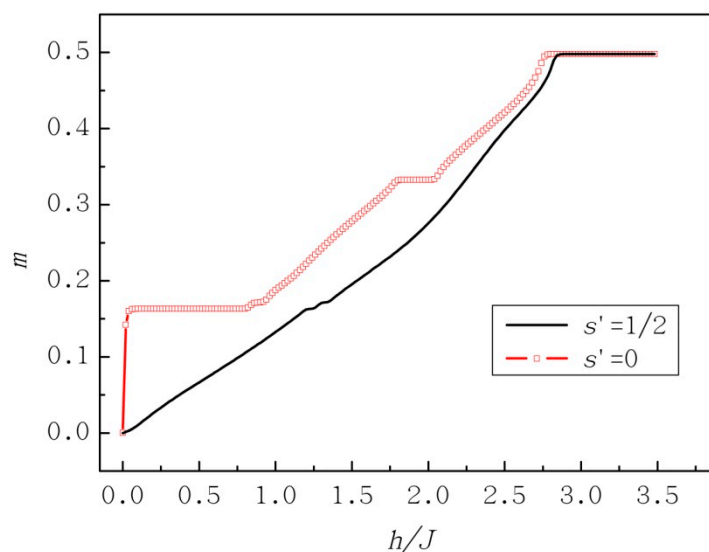

Figure 8. Field dependence of magnetization *m* for the system of Figure 1c (QMC; *T* = 0.01 *J*).

Similar calculations were performed also for the model "sandwich" structure shown in Figure 2. The results of the QMC study for the case *s′* = 1/2 are shown in Figure 9 and demonstrate intermediate magnetization plateau at *m* = 1/18 for structure Figure 4a and *m* = 1/26 for structure Figure 4b in agreement with the suggested existence of the energy gap for the excitations with $S \geq S_0$ (similar to the magnetic derivative of the nanoribbons considered above).
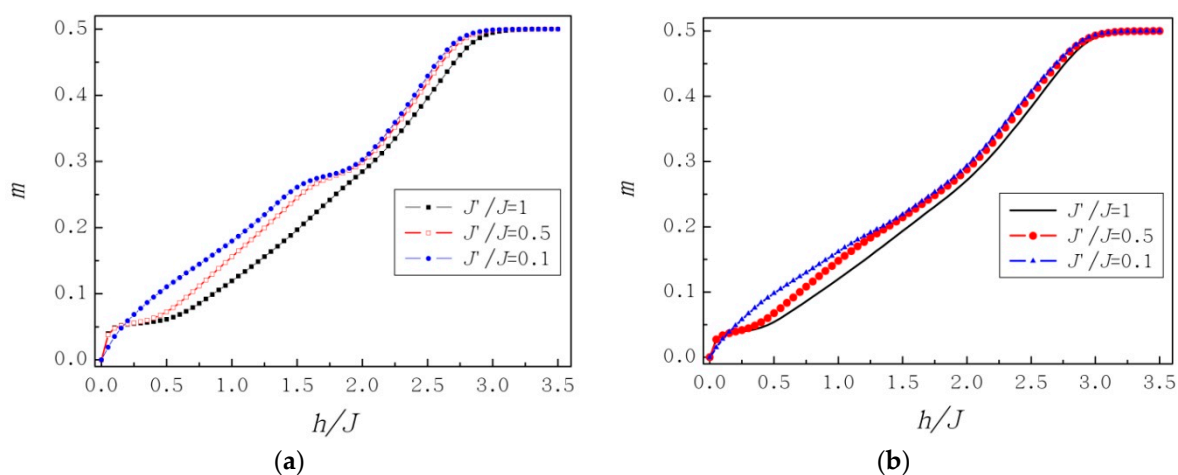

Figure 9. Field dependence of magnetization at different values of coupling between nanoribbons and embedded transition metal ions for the structures Figure 4a,b, respectively (QMC; *T* = 0.01 *J*). (**a**) N_{spins} = 900, (**b**) N_{spins} = 800.

Despite the frustrated character of chain spin structure formed by triangular graphenic clusters, in the case of a weak interaction between the triangular fragments and embedded transition metal

ions the analytical perturbation theory permits us to treat it as an effective bipartite spin system. Thus, using this technique [42,43], we derived the following low-energy effective Hamiltonian:

$$\mathbf{H}_{eff} = J_{eff} \sum_{m=1}^{L-1} S_{1,m}(S_{2,m} + S_{2,m+1}), \quad J_{eff} = J'_1 \rho_1 + 2J'_2 \rho_2 ,$$
$$\rho_i = \langle \Psi_0(S_0)|S_i^z|\Psi_0(S_0)\rangle / S_0$$

where the coupling constants J'_1 and J'_2 correspond to the interactions between transition metal ion and nearest and next nearest carbon atoms of the triangular clusters.

At $J'_2 = 0$ the spin lattice system shown in Figure 4 has an alternant character. Therefore, according to the extended Lieb theorem it has macroscopic ground state spin in thermodynamic limit.

The effective coupling constant changes its sign when the ratio $R = J'_2/J'_1$ passes the critical value:

$$R_c = -\rho_1/(2\rho_2) > 0$$

This means that the increase of J'_2 leads to the macroscopic jump in the value of the ground state spin (spin switching) when the ratio of coupling constants R passes through the critical value R_c. This analysis is valid for triangular clusters of arbitrary size. For the predictions of the appearance of spin switching only the numerical estimations for the reduced spin densities ρ_1 and ρ_2 are required. Thus, for the triangular graphitic clusters formed by 13 spins (Figure 4) the exact diagonalization gives the estimate of $R_c \approx 0.333$.

4. Discussion

We studied analytically and numerically the energy spectrum and low-temperature magnetic properties of quantum Heisenberg spin models for narrow graphitic nanoribbons with periodically embedded heteroatoms and the chain systems on the base of small graphitic clusters connected by bridge atoms of transition metals: components of hypothetical quasi-one-dimensional crystals. For several nanoribbon structures with embedded heteroatoms we found macroscopic ground state spin, gapless lowest excitation spectra and intermediate magnetization plateaus at low temperatures. On the base of DMRG and QMC calculations, we demonstrated the existence of a small gap in the energy spectrum of polyacene, the simplest representation of zigzag nanoribbons. This result is in agreement with DMRG calculations for the Hubbard model [15] and DFT simulation [12]. On the other hand, our analytical LSWA approach shows a gapless excitation spectrum. The disagreement with the DMRG consideration emphasizes the importance of carefully accounting for electron correlation effects for the adequate simulation of the magnetic properties of graphene-based materials.

On the base of our numerical simulation we found the intermediate plateau in field dependence of pristine polyacene magnetization is present at low temperatures. This plateau is also present in field dependence of magnetization of magnetic derivatives of polyacene and is absent in the case of polyphenylene. It should be interesting to check this effect experimentally by measuring the corresponding magnetization profile at low temperatures.

We also demonstrated the possibility of spin switching for frustrated systems on the base of triangular graphitic clusters connected by bridged ions of transition metals and analyzed the necessary conditions for the realization of this effect. This effect may be used for the design of magnetic chemo-sensors because the changes in chemicals surrounding of our material may change drastically the ratio of coupling constants R describing the interactions between triangular nanoflake and group of atoms with nonzero total spin, e.g., complex cation of the transition metal.

Note also, the provided computations were used for such a search bearing in mind that the existing solid-state quantum chemistry packages related to electron simulation of magnetic properties of crystals do not provide, an option of including linear spin waves and thus have restricted capacity in the sense of modeling temperature-dependent responses of the target materials to the magnetic field and other similar properties. Thus, the present analysis indicates to a necessity of widening the

repertory of possible quantum states to be included in the modeling of crystals which will be possibly done in the future.

Appendix A. Linear Spin Wave Approximation for Zigzag Nanoribbons

Spin Hamiltonian for polyacene with embedded heteroatoms (Figure 1a) may be written as:

$$\hat{\mathbf{H}} = \sum_{l=1}^{N} [S_{1l}(S_{2l} + S_{2l+1}) + S_{2l}S_{3l} + \alpha S_{4l}(S_{3l} + S_{3l+1})] \tag{A1}$$

Here we assume the periodic boundaries $S_{2N+1} = S_{21}$, $S_{3N+1} = S_{31}$, and an arbitrary value of the embedded spin $S_{4l} = s'$.

In the spin wave approximation the corresponding linearized Hamiltonian had the form:

$$\hat{\mathbf{H}}_0 = E_{AF} + \sum_{l=1}^{N} \left\{ \frac{1}{2}\left(2a_{1,l}^\dagger a_{1,l} + 3a_{2,l}^\dagger a_{2,l}\right) + \left(\frac{1}{2} + 2\alpha s'\right)a_{3,l}^\dagger a_{3,l} + \alpha a_{4,l}^\dagger a_{4,l} + \right.$$
$$\left. + \frac{1}{2}\left[a_{1,l}^\dagger(a_{2,l}^\dagger + a_{2,l+1}^\dagger) + a_{2,l}^\dagger a_{3,l}^\dagger + h.c.\right] + \alpha \sqrt{\frac{s'}{2}} a_{4,l}^\dagger\left[(a_{3,l}^\dagger + a_{3,l+1}^\dagger) + h.c.\right] \right\} \tag{A2}$$
$$E_{AF} = -\left(\frac{3}{4} + 2\alpha s'\right)N.$$

Translation symmetry in the horizontal direction permitted us to introduce a quasi-wave vector $k = 2\pi l/N$, $l = 0, 1, \ldots, N-1$, and to perform Fourier-transform for operators

$$a_{jl} = \frac{1}{\sqrt{N}}\sum_{k} \exp(ikx)a_{jk}, \ j = 1, 3;$$
$$a_{jl} = \frac{1}{\sqrt{N}}\sum_{k} \exp(-ikx)a_{jk}, \ j = 2, 4; \tag{A3}$$

After the Fourier-transform the Hamiltonian (A3) took the form:

$$\hat{\mathbf{H}}_0 = E_{AF} + \sum_{k} \left\{ \frac{1}{2}\left(2a_{1k}^\dagger a_{1k} + 3a_{2k}^\dagger a_{2k}\right) + \left(\frac{1}{2} + 2\alpha s'\right)a_{3k}^\dagger a_{3k} + \alpha a_{4k}^\dagger a_{4k} + \right.$$
$$\left. + \frac{1}{2}\left[(1 + e^{ik})a_{1k}^\dagger a_{2k}^\dagger + a_{2k}^\dagger a_{3k}^\dagger\right] + \alpha \sqrt{\frac{s'}{2}}(1 + e^{-ik})a_{3k}^\dagger a_{4k}^\dagger + h.c. \right\} \tag{A4}$$

To diagonalize (A4) we used the Heisenberg representation of the creation and annihilation operators in order to derive the equations of motion:

$$\dot{a}_{jk} = \frac{i}{\hbar}\left[\hat{\mathbf{H}}, a_{jk}\right],$$

and applied the generalized *u-v* Bogolubov transformation in the form:

$$a_{jk} = \sum_{i=1}^{4}\left(U_{ik}^{(j)}b_{ik} + V_{ik}^{(j)*}b_{ik}^\dagger\right), \ j = 1-4,$$

assuming that the new set of operators diagonalizes the Hamiltonian (A4). In the result, we had:

$$\dot{b}_{jk} = -\frac{i}{\hbar}\varepsilon_{jk}b_{jk}$$

For each ε_{jk} we had similar sets of eight linear uniform algebraic equations for eight coefficients, which separated into two sets with four equations each, corresponding to four energy branches with the dispersion relations:

$$\left[(\varepsilon \mp 1)(\varepsilon \pm 3/2) + \cos^2\tfrac{k}{2}\right]\left[(\varepsilon \pm \alpha)(\varepsilon \mp 1/2 \mp 2\alpha s') + 2\alpha^2 s'\cos^2\tfrac{k}{2}\right]+ \\ +\tfrac{1}{4}(\varepsilon \mp 1)(\varepsilon \pm \alpha) = 0 \tag{A5}$$

One should take only non-negative solutions for ε (energies) in (A5). It is easy to show that at $k = 0$ the solution $\varepsilon = 0$ always exists. This means that in the linear spin wave approximation the energy spectrum is gapless for any value of s' and coupling parameter α.

In the long-wave limit $k << 1$ the approximate formulas for the lowest energies are different for the cases $s' \neq 1/2$ and $s' = 1/2$

$$s' \neq \frac{1}{2}: \quad \varepsilon_k \approx \frac{(2\alpha s' + 1)}{4|2s' - 1|}k^2 \tag{A6}$$

and

$$s' = \frac{1}{2}: \quad \varepsilon_k \approx \frac{1}{2}\sqrt{\alpha}|k| \tag{A7}$$

Similar calculations for 3-zigzag nanoribbon structures also gave the gapless energy spectrum:

$$s' \neq \frac{1}{2}: \quad \varepsilon_k \approx \frac{(\alpha s' + 1)}{2|2s' - 1|}k^2 \tag{A8}$$

and:

$$s' = \frac{1}{2}: \quad \varepsilon_k \approx \frac{1}{2}\sqrt{\frac{\alpha(\alpha + 2)}{(2\alpha + 1)}}|k| \tag{A9}$$

References

1. Slota, M.; Keerthi, A.; Myers, W.K.; Tretyakov, E.; Baumgarten, M.; Ardavan, A.; Sadeghi, H.; Lambert, C.J.; Narita, A.; Müllen, K.; et al. Magnetic esge states and coherent manipulation of graphene nanoribbons. *Nature* **2018**, *557*, 691–696. [CrossRef] [PubMed]
2. Salemi, L.; Lherbier, A.; Charlier, J.-C. Spin-dependent properties in zigzag graphene nanoribbons with phenul-edge defects. *Phys. Rev. B* **2018**, *98*, 214204. [CrossRef]
3. Hoffmann, R.; Kabanov, A.A.; Golov, A.A.; Proserpio, D.M. Homo Citans and Carbon Allotropes: For an Ethics of Citations. *Angew. Chem. Int. Ed.* **2016**, *55*, 10962. [CrossRef] [PubMed]
4. Görne, A.L.; Dronskowski, R. Covalent bonding versus total energy: On the attainability of certain predicted low-energy carbon allotropes. *Carbon* **2019**, *148*, 151–158. [CrossRef]
5. Samara Carbon Allotrope Database (SACADA). Available online: http://sacada.sctms.ru/ (accessed on 10 May 2019).
6. Misurkin, I.A.; Ovchinnikov, A.A. The electronic structures and properties of polymeric molecules with conjugated bonds. *Usp. Khim.* **1977**, *46*, 1835–1870. (In Russian) [CrossRef]
7. Ovchinnikov, A.A.; Shamovsky, I.L. The structure of the ferromagnetic phase of carbon. *J. Mol. Struct. Theochem.* **1991**, *251*, 133–140. [CrossRef]
8. Tchougréeff, A.L.; Hoffmann, R. Charge and Spin Density Waves in the Electronic Structure of Graphite. Application to Analysis of STM Images. *J. Phys. Chem.* **1992**, *96*, 8993–8998. [CrossRef]
9. Fujita, M.; Wakabayashi, K.; Nakada, K.; Kusakabe, K. Peculiar localized state at zigzag graphite edge. *J. Phys. Soc. Jap.* **1996**, *65*, 1920–1923. [CrossRef]
10. Wakabayashi, K.; Fujita, M.; Ajiki, H.; Sigrist, M. Electronic and magnetic properties of nanographite ribbons. *Phys. Rev. B* **1999**, *59*, 8271–8282. [CrossRef]

11. Yamashiro, A.; Shimoi, Y.; Harigaya, K.; Wakabayashi, K. Spin- and charge-polarized states in nanographene ribbons with zigzag edges. *Phys. Rev. B* **2003**, *68*, 193410. [CrossRef]

12. Son, Y.-W.; Cohen, M.L.; Louie, S.G. Energy gap in graphene nanoribbons. *Phys. Rev. Lett.* **2006**, *97*, 2016803. [CrossRef] [PubMed]

13. Lieb, E.H. Two theorems on the Hubbard model. *Phys. Rev. Lett.* **1989**, *62*, 1201–1204. [CrossRef]

14. Felder, H.; Meng, Z.Y.; Lang, T.C.; Assaad, F.F.; Wessel, S.; Honecker, A. Dynamical signatures of edge-state magnetism on graphene nanoribbons. *Phys. Rev. Lett.* **2011**, *106*, 226401. [CrossRef] [PubMed]

15. Hikihara, T.; Hu, X.; Lin, H.; Mou, C.-Y. Ground state properties of nanographite systems with zigzag edges. *Phys. Rev. B* **2003**, *68*, 035432. [CrossRef]

16. Golor, M.; Lang, T.C.; Wessel, S. Quantum Monte Carlo studies of edge magnetism in chiral graphene nanoribbons. *Phys. Rev. B* **2013**, *87*, 155441. [CrossRef]

17. Golor, M.; Wessel, S.; Schmidt, M.J. Quantum natire of edge magnetism in graphene. *Phys. Rev. Lett.* **2014**, *112*, 046601. [CrossRef] [PubMed]

18. Yu, G.; Lü, X.; Jiang, L.; Gao, W.; Zheng, Y. Structural, electronic and magnetic properties of transition-metal embedded zigzag-enged graphene nanoribbons. *J. Phys. D* **2013**, *46*, 375303. [CrossRef]

19. Yang, S.; Li, J.; Li, S.-S. Antiferromagnetic-ferromagnetic transition in zigzag graphene nanoribbons indused by substitutional doping. *Chin. Phys.* **2018**, *27*, 117102. [CrossRef]

20. Kan, M.; Zhou, J.; Li, Y.; Sun, Q. Using carbon chains to mediate magnetic coupling in zigzag graphene nanoribbons. *Appl. Phys. Lett.* **2012**, *100*, 173106. [CrossRef]

21. Zhou, J.; Wang, Q.; Sun, Q.; Jena, P. Intinsic ferromagnetism in two-dimensional carbon structures: Triangular graphene nanoflakes linked by carbon chains. *Phys. Rev. B* **2011**, *84*. [CrossRef]

22. Wang, W.L.; Meng, S.; Kaxiras, E. Graphene nanoflakes with large spin. *Nano Lett.* **2008**, *8*, 241–245. [CrossRef]

23. Bulaevskii, L.N. Quasihomopolar electron levels in crystalls and molecules. *Z. Eksp. Teor. Fiz.* **1966**, *51*, 230–239.

24. Ovchinnikov, A.A. Multiplicity of the ground state of large alternant organic molecules with cojugated bonds (Do Organic Ferromagnetics Exist?). *Theor. Chim. Acta* **1978**, *47*, 297–304. [CrossRef]

25. Klein, D.J.; Nelin, C.J.; Alexander, S.A. High-spin hydrocarbons. *J. Chem. Phys.* **1982**, *77*, 3101–3108. [CrossRef]

26. Klein, D.J.; Alexander, S.A. Organic polyradicals, high-spin hydrocarbons, and organic ferromagnets. *Stud. Phys. Theor. Chem.* **1987**, *51*, 404–419.

27. Cheranovskii, V.O. Spin permutation tecnique in the theory of strongly correlated electron systems. In *Valence Bond Theory*; Cooper, D.L., Ed.; Elsevier: Amsterdam, The Netherlands, 2002; pp. 699–727.

28. Tchougréeff, A.L. Several Stories from Theoretical Chemistry with some Russian Flavor and Implications for Theorems of Chemistry, Vagueness of Its Concepts, Fuzziness of Its Definitions, Iconicity of Its Language, and Peculiarities of Its Nomenclature. *Int. J. Quant. Chem.* **2016**, *116*, 137–160. [CrossRef]

29. Plekhanov, E.A.; Tchougréeff, A.L. Resonating Valence Bonds in Chemistry and Solid State. In *Handbook of Inorganic Chemistry*; Dronskowski, R., Kikkawa, S., Stein, A., Eds.; Wiley Interscience: New York, NY, USA, 2017; Chapther 4; Volume 5.

30. White, S.R. Density matrix formulation for quantum renormalization groups. *Phys. Rev. Lett.* **1992**, *69*, 2863–2866. [CrossRef]

31. Sandvik, A.W. Stochastic series expansion method with operator-loop update. *Phys. Rev. B* **1999**, *59*, R14157–R14160. [CrossRef]

32. Lieb, E.H.; Mattis, D.C. Ordering energy levels of interacting spin systems. *J. Math. Phys.* **1962**, *3*, 749–751. [CrossRef]

33. Klein, D.J. Ground state features for Heisenberg models. *J. Chem. Phys.* **1982**, *77*, 3098–3100. [CrossRef]

34. Lieb, E.; Shoultz, T.; Mattis, D. Two soluble models of an antiferromagnetic chain. *Ann. Phys.* **1961**, *16*, 407–466. [CrossRef]

35. Ovchinnikov, A.A.; Cheranovskii, V.O. On the excitation spectrum of alternant magnetic chains with odd number of atoms in elementary cell. *Dokl. Akad. Nauk SSSR* **1982**, *266*, 838–840.

36. Affleck, I.; Lieb, E.H. A proof of part of Haldane's conjecture on spin chains. *Lett. Math.Phys.* **1986**, *12*, 57–69. [CrossRef]

37. Fukui, T.; Kawakami, N. Spin chain with periodic array of impurities. *Phys. Rev. B* **1997**, *55*, R14709–R14712. [CrossRef]

38. Cheranovskii, V.O.; Özkan, I. The ground state spin ordering and lowest energy excitations of a model organic ferrimagnet-polyallyl spin chain. *J. Mag. Mag. Mater.* **2001**, *223*, 156–162. [CrossRef]

39. Nasu, K. Periodic Kondo-Hubbard model for a quasi-one-dimensional organic ferromagnet *m*-polydiphenilcarbene: Cooperation between electron correlation and topological structure. *Phys. Rev. B* **1986**, *33*, 330–338. [CrossRef]

40. Goodenough, J.B. *Magnetism and the Chemical Bond*; Interscience-Wiley: New York, NY, USA, 1963.

41. Slavin, V.V.; Krivchikov, A.A. Magnetic properties of the quantum Shastry–Sutherland model with spin S = $\frac{1}{2}$. *Low Temp. Phys.* **2014**, *40*, 985–989. [CrossRef]

42. Ovchinnikov, A.A.; Cheranovskii, V.O. Perturbation theory in the spin Hamiltonian methods. *Theor. Exp. Chem.* **1980**, *16*, 119–120. [CrossRef]

43. Cheranovskii, V.O.; Ezerskaya, E.V.; Klein, D.J.; Kravchenko, A.A. Magnetic properties of model non-carbon nanotubes with macroscopic value of ground spin. *J. Mag. Mag. Mater.* **2011**, *323*, 1636–1642. [CrossRef]